PHYSICAL REVIEW D **79,** 014502 (2009)

Bottom baryons from a dynamical lattice QCD simulation

Randy Lewis
Department of Physics and Astronomy, York University, Toronto, Ontario, Canada M3J 1P3

R. M. Woloshyn
TRIUMF, 4004 Wesbrook Mall, Vancouver, British Columbia, Canada V6T 2A3
(Received 7 July 2008; revised manuscript received 17 November 2008; published 7 January 2009)

Bottom baryon masses are calculated based on a 2 + 1 flavor dynamical lattice QCD simulation. The gauge field configurations were computed by the CP-PACS and JLQCD collaborations using an improved clover action. The bottom quark is described using lattice NRQCD. Results are presented for single and double-b baryons at one lattice spacing. Comparison with experimental values is discussed.

DOI: 10.1103/PhysRevD.79.014502 PACS numbers: 12.38.Gc, 14.20.Mr

I. INTRODUCTION

There have been a number of developments since our previous systematic study [1] of heavy baryons in quenched lattice QCD which suggest to us to revisit this problem. On the experimental side, masses of four bottom baryons have been measured since our earlier work. On the theory side improved analysis methods should allow for a more precise determination of the masses and subsequently a more stringent test of the calculation. As well, full dynamical simulations are becoming the norm. Dynamical simulations for heavy baryons using lattice formulations different from that used in this work have been reported in Refs. [2,3].

Besides lattice QCD, heavy baryons have been studied in many other approaches. A few recent papers (from which the extensive earlier literature may be traced) include work on QCD sum rules [4], the quark model [5,6] and the combined heavy quark and $1/N_c$ expansions [7].

With a single b-quark and different flavor and spin combinations of up, down, and strange quarks eight different baryons can be constructed. The properties of the baryons are summarized in Table I. For the purposes of this work exact isospin symmetry is assumed; u and d quarks are taken to be degenerate. The experimental values for masses of Σ_b, Σ_b^*, Ω_b, and Ξ_b have only become available in the past year [9–11].

A variety of approaches are being pursued to incorporate dynamical quark effects in lattice QCD simulations. Ideally one would like to have u/d and strange (2 + 1 flavor) dynamical effects. As well, the light quarks (u/d) should have small masses and the lattice volume should be large. It is clear that these requirements stress the computing resources available to even the largest lattice QCD collaborations so some compromises have to be made. It is not feasible for us to generate our own dynamical gauge field configurations. Instead, 2 + 1 flavor dynamical configurations, made available by the CP-PACS and JLQCD collaborations [12,13], were used. These are based on the Iwasaki RG gauge field action [14] and an improved clover action [15] for the quarks.

Lattice NRQCD [16] is used for the heavy quark. For the lattice spacing considered here, only the b quark is heavy enough for its mass to lie above the cutoff scale. Charm is too light to be simulated by NRQCD and so, unlike Ref. [1], charmed baryons are not considered in this study.

The parameters in the calculation, namely, u/d, s and b-quark masses as well as the overall scale, are fixed by calculations done in the meson sector. Masses of heavy baryons are then predictions of the simulation. In addition to single-b baryons listed in Table I we also calculate the masses of the double-b baryons with properties given in Table II. At present there are no data for double-b baryons but it is hoped that eventually they will be observed in some future experiment.

In Sec. II details of the simulation are presented. There is a brief summary of the actions and the lattice parameters. The analysis method is also discussed.

Results are given in Sec. III and compared to available experimental data. Limitations of this work and future directions are discussed in Sec. IV.

TABLE I. Properties of single-b baryons showing valence content (q = u/d), spin parity, isospin, and mass (in GeV). The quantity s_l is the total spin of the light quark pair.

baryon	quark content	J^P	I	s_l	mass	Ref.
Λ_b	qqb	$\frac{1}{2}^+$	0	0	5.624	[8]
Σ_b	qqb	$\frac{1}{2}^+$	1	1	5.812(3)	[9]
Σ_b^*	qqb	$\frac{3}{2}^+$	1	1	5.8133(3)	[9]
Ω_b	ssb	$\frac{1}{2}^+$	0	1	6.165(16)	[10]
Ω_b^*	ssb	$\frac{3}{2}^+$	0	1		
Ξ_b	qsb	$\frac{1}{2}^+$	$\frac{1}{2}$	0	5.793(3)	[11]
Ξ_b'	qsb	$\frac{1}{2}^+$	$\frac{1}{2}$	1		
Ξ_b^*	qsb	$\frac{3}{2}^+$	$\frac{1}{2}$	1		

TABLE II. Properties of double-b baryons showing valence content ($q = u/d$), spin parity and isospin.

Baryon	quark content	J^P	I
Ξ_{bb}	qbb	$\frac{1}{2}^+$	$\frac{1}{2}$
Ξ^*_{bb}	qbb	$\frac{3}{2}^+$	$\frac{1}{2}$
Ω_{bb}	sbb	$\frac{1}{2}^+$	0
Ω^*_{bb}	sbb	$\frac{3}{2}^+$	0

II. NUMERICAL SIMULATION

A. Simulation details

Gauge field configurations incorporating the full dynamical vacuum polarization effects of u, d, and s quarks are employed in this work. These gauge configurations were generated by the CP-PACS and JLQCD collaborations [12,13] and made available through the Japan Lattice Data Grid [17].

The gauge field action is an improved action developed by Iwasaki [14] and in addition to the standard plaquette term it contains six-link operators with coefficients tuned so that the action lies close to the renormalized trajectory. The quark action is of the clover type [15]. The coefficient of the clover was tuned nonperturbatively [18] and is the same for all values of sea-quark mass. Hybrid Monte Carlo was used for the two light flavors (u/d) and the polynomial hybrid Monte Carlo was used for the strange sea quark [19].

In this work, a subset of the CP-PACS/JLQCD 2 + 1 flavor configurations at $\beta = 1.90$ with lattice size $20^3 \times 40$ is used. The coefficient of the clover term in the quark action was 1.715 (see Ref. [13]). Other lattice parameters are given in Table III. The quantity U_0 equals $1/3$ of the trace of the mean gauge-field link in Landau gauge and is used as the tadpole factor in the NRQCD action.

A nonrelativistic action [16] is used to describe the b quark. This approach is useful when the bare mass of the quark is larger than the cutoff scale. The particular form of the action used in this work is essentially the same as that used in our previous works [1,20]. Terms up to $\mathcal{O}(1/M_0^3)$ in the heavy quark mass M_0 are retained. The only difference is that while [1,20] used an anisotropic lattice, here the lattice is isotropic. The details of the action are given in the appendix.

TABLE III. Lattice parameters. The lattice size is $20^3 \times 40$ with Iwasaki gauge action $\beta = 1.90$ and quark action clover coefficient $c_{\mathrm{SW}} = 1.715$. The masses of u/d and s quarks are encoded in the hopping parameters κ_q and κ_s, respectively.

configurations	κ_q	κ_s	U_0
480	0.1358	0.1358	0.8396
576	0.1364	0.1358	0.8415
576	0.1368	0.1358	0.8425
576	0.1370	0.1358	0.8432
480	0.1358	0.1364	0.8405
576	0.1364	0.1364	0.8422
576	0.1368	0.1364	0.8433
576	0.1370	0.1364	0.8439

Simulations were done for three values of the heavy-quark bare mass: 2.28, 2.34, and 2.40 in lattice units. This allowed for interpolation to the physical b-mass value.

Correlation functions were calculated using local hadron operators at the source and sink. For heavy baryons the operators used were exactly the same as detailed in Ref. [1]. In addition to baryon correlators, correlators were calculated for pseudoscalar and vector mesons in the light sector (u/d, s), the heavy-light sector (B-mesons) and the heavy-heavy sector (Υ). The meson calculations were used to determine the "physical" values for the quark masses and the overall scale. As well they provide some additional predictions which test the calculation.

Nonrelativistic quarks propagate only forward in time. For combining relativistic quarks with nonrelativistic quarks it is convenient to use Dirichlet boundary conditions for the light quark propagators; propagation across the time boundary is not allowed. If the source time is set in from the time boundary (four time steps is used in this calculation) it can be verified that meson masses in the light sector are the same, within statistical errors, as those computed with more usual periodic time boundary conditions.

In order to get some extra suppression of statistical fluctuations and reach the level of precision that we would like, multiple sources were used. For each gauge field configuration a set of correlators was calculated using different space-time points as the source point. This set was averaged and the average value was used as the representative correlation function for the configuration. Eight sources per configuration were used in this calculation.

B. Analysis

Correlation functions were fit with a sum of exponentials

$$g(t) = \sum_{i=0}^{n-1} z_i e^{-E_i t} \tag{1}$$

over a fixed time range which for our standard analysis extended for 27 time steps starting one time step past the source position. For mesons three exponential terms were found to be adequate while for baryons four terms were used. The advantage of a multiexponential fit over methods such as fitting over an "effective mass" plateau is that it is less subjective. Also it makes better use of the correlation function data at times where the statistical error is small.

To stabilize the fits, a constrained fitting method [21] was used. The usual χ^2 is augmented with a term which acts to prevent the fit parameters from straying outside some sensible (but broad) range. The constraint term for the coefficients z_i was taken to be

$$\sum_{i=0}^{n-1} \frac{(z_i - \bar{z}_i)^2}{\sigma^2_{\bar{z}_i}}. \tag{2}$$

The priors were chosen to be $\bar{z}_i = \sigma_{\bar{z}_i} = g(0)/n$, which is a very loose constraint. The constraint term for the exponents (energies) has a similar form

$$\sum_{i=0}^{n-1} \frac{(E_i - \bar{E}_i)^2}{\sigma^2_{\bar{E}_i}}. \tag{3}$$

One might be tempted to choose a constraint which is minimally biased, such as equal spacing of the energies $\bar{E}_i - \bar{E}_{i-1} = \delta E$ and $\sigma_{\bar{E}_i} = \delta E$. In practice it was found that to prevent the occurrence of obviously spurious solutions, where, for example, two terms have the same exponent and coefficients of opposite sign, a somewhat tighter constraint is needed. For our fits we use $\bar{E}_1 - \bar{E}_0 = 0.5$ and $\bar{E}_i - \bar{E}_{i-1} = 1.0$, $i > 1$ with $\bar{E}_0$ equal to 0.5 for mesons and 0.8 for baryons. The $\sigma_{\bar{E}_i}$ were chosen to be proportional to the spacing between the $\bar{E}_i$ with a common reduction factor taken to be 0.83. With this setup spurious solutions were avoided and the ground state energy was very stable with respect to changes in the constraint parameters. For example, it was found that changing prior parameters by 20% led to changes in single-b baryon simulation energies (which are most sensitive) of about 1%. This effect is incorporated into the estimated systematic uncertainty.

To determine the statistical errors, bootstrap analysis was used. A sample of 600 bootstrap ensembles was created and a complete analysis was carried out for each ensemble. In this way the uncertainty in determining the quark mass parameters and the scale is incorporated into the bootstrap error estimate of the final result.

A few systematic effects were examined explicitly. These include sensitivity to the choice of time range for fitting the correlators, to the determination of the b-quark mass and to the choice of extrapolation function in u/d and s quark mass. In addition, there are systematic errors associated with the omitted higher order effects in the NRQCD action. These are discussed in great detail by Gray *et al.* [22] for the Υ system. For heavy-light hadrons the appropriate power counting is different than for quarkonium [23]. The expansion parameter is p/M_0 where the typical momentum of the heavy quark $p \sim \Lambda_{\mathrm{QCD}}$, independent of quark mass. Radiative corrections to the action then are $\mathcal{O}(\alpha_s \Lambda_{\mathrm{QCD}}/M_0)$ relative to the leading kinetic term [23] which we estimate can induce a 1.5% relative uncertainty in the simulation energies. The NRQCD action is corrected for $\mathcal{O}(a^2)$ lattice spacing errors at tree level. The leading discretization corrections are $\mathcal{O}(\alpha_s (a\Lambda_{\mathrm{QCD}})^2)$ and a 0.5% fractional systematic error is assigned to these effects. The action used in this work includes $\mathcal{O}(1/M_0^3)$ terms and higher order relativistic effects are assumed to be negligible.

III. RESULTS

A. Mesons

The first task is to determine the quark mass parameters and overall scale. We start with the u/d and s sector and use the pion, rho meson, and phi meson masses as experimental input. Lattice masses for these mesons are calculated with the eight ensembles in Table III. For each correlator the valence mass was taken to be equal to the u/d mass or to the strange mass. No partially quenched correlators, with a valence mass different from a sea-quark mass of the same flavor were used in this work.

The lattice meson masses were then fit as a function of quark mass using the vector Ward identity (VWI) definition of the quark mass $m = (1/\kappa - 1/\kappa_{\mathrm{cr}})/2$ where κ_{cr} is the point where the pseudoscalar meson mass vanishes when all valence and sea-quark masses have this hopping parameter.

The fitting functions are motivated by the study of light quark masses in Ref. [13]. For the pseudoscalar meson (with degenerate valence quarks) it was found that the three terms

$$b_1 m_v + b_2(2m_q + m_s) + b_3 m_v(2m_q + m_s), \tag{4}$$

where m_v, m_q, and m_s are valence, u/d, and s quark masses from the VWI definition, gives a good description of the mass squared lattice data. Note that κ_{cr} is a free parameter in the fit as are the coefficients b_1, b_2, b_3.

For the vector meson the mass was fit using

$$c_1 + c_2 m_v + c_3(2m_q + m_s) + c_4 m_v^2 \tag{5}$$

which takes into account a slight nonlinear dependence on the quark mass. In determining the coefficients of this fit κ_{cr} is fixed to the value obtained in the pseudoscalar meson fit.

After the fit parameters are determined one can solve for the values of the hopping parameters and the lattice spacing that reproduce the input experimental numbers. The results are $\kappa_q = 0.137\,84(2)$ and $\kappa_s = 0.136\,18(9)$ with a value of the inverse lattice spacing $a^{-1} = 1.89(3)$ GeV. We note that the inverse lattice spacing obtained here is slightly different from that quoted in [13] but it has to be remembered that the number of configurations, the number of ensembles and the details of the mass extrapolation are also different.

The b-quark mass is determined using the Υ mass as input. In NRQCD the quark mass has been removed from the action. The zero-momentum hadron correlator yields a simulation energy to which the renormalized quark mass and energy shift must be added to get the hadron mass. Alternatively the hadron mass can be determined from the kinetic energy. For this purpose the correlators for $b\bar{b}$

mesons carrying a unit of momentum were calculated. The meson mass M (lattice units) is obtained using

$$M = \frac{2\pi^2}{N_s^2(E_{\mathrm{sim}}(p) - E_{\mathrm{sim}}(0))} \tag{6}$$

where N_s is the spatial extent of the lattice, $p = 2\pi/N_s$ and the difference in simulation energies is just the kinetic energy.

Kinetic energies were calculated for Υ at all the heavy bare quark masses listed in Sec. II A and for all eight ensembles. It was found that kinetic energies were practically independent of the values of the sea-quark masses with no systematic trend which would allow for extrapolation. Therefore for each ensemble an independent determination of the bare b-quark mass was made by inputting the experimental Υ mass and the inverse lattice spacing obtained above. The values (in lattice units) varied in the small range from 2.375(78) to 2.416(77). A value in the middle of this range 2.391(78), obtained from the ensemble $\kappa_q = 0.1368$, $\kappa_s = 0.1364$, was used as our nominal value for the b mass. The maximum and minimum values were used to estimate a systematic uncertainty in the hadron masses. The effect of choosing different values for the b-quark mass was found to be small, typically changing the final hadron mass by an MeV or so.

Having determined the physical point for the b-quark mass one can get the splitting between the Υ and the η_b just from interpolating the difference in simulation energies for the $b\bar{b}$ vector and pseudoscalar channels. The calculated $\Upsilon - \eta_b$ mass difference is given in Table IV and is smaller than the recent value reported by the *BABAR* collaboration [24]. The underestimate of the quarkonium spin splitting has been a common feature of simulations done with NRQCD [25–27]. The systematic study by Gray *et al.* [22] (see their Fig. 14) shows that this quantity is quite sensitive to the continuum extrapolation for light sea-quark masses. Gray *et al.* [22] predicted a continuum extrapolated value of 61(14) MeV, somewhat larger than our value at a nonzero lattice spacing. Note that part of the difference between their value and ours is due to $\mathcal{O}(v^6)$ terms in the NRQCD action which we include and they do not. From a test run on a single ensemble it is estimated that these terms decrease the spin splitting by about 15%.

TABLE IV. Lattice results for meson masses and spin splittings (in GeV) compared to experimental values. The $\Upsilon - \eta_b$ result is from [24], other experimental values are from [8].

	mass-$M_\Upsilon/2$	mass	Experiment
$\Upsilon - \eta_b$		$0.039(1)(^{8}_{7})$	$0.0714(^{31}_{23})(27)$
B	0.527(6)(8)	5.257(6)(8)	5.2793(4)
B^*	$0.530(7)(^{10}_{9})$	$5.300(7)(^{10}_{9})$	5.325(1)
B_s	0.617(3)(10)	5.346(3)(10)	5.366(1)
B_s^*	0.658(4)(11)	5.388(4)(11)	5.412(1)
$B^* - B$		$0.043(3)(^{5}_{4})$	0.0458(4)
$B_s^* - B_s$		$0.042(2)(^{5}_{4})$	0.0461(15)

Although the main motivation for this work was to study heavy baryons, the masses for heavy-light (B) mesons were also calculated. The masses were computed relative to the Υ which was an input to the calculation. Above, the kinetic energy was used to determine the Υ mass but alternatively it is given as $M_\Upsilon = E_{\mathrm{sim}}^{(\Upsilon)} + 2(ZM_0 - E_{\mathrm{shift}})$ where Z is the mass renormalization factor and E_{shift} is an additive mass shift. The quantities Z and E_{shift} are independent of the hadronic state [28] so for a hadron, such as the B-meson, containing a single b quark $M_B = E_{\mathrm{sim}}^{(B)} + ZM_0 - E_{\mathrm{shift}}$. The mass can then be obtained using

$$M_B = E_{\mathrm{sim}}^{(B)} + \tfrac{1}{2}(M_\Upsilon - E_{\mathrm{sim}}^{(\Upsilon)}). \tag{7}$$

The results, extrapolated in light quark mass and converted to physical units, are shown in Table IV along with the experimental values from the PDG [8]. The first error in the lattice results is the statistical (bootstrap) error. The second error incorporates the changes that result from changes in the time range used in fitting the correlators, the uncertainty in determining the b-quark mass and the choice of u/d and s-quark mass fitting function. For the mass range used in this present simulation the heavy-light meson masses are consistent with a linear dependence on quark mass

$$c_1 + c_2 m_v + c_3(2m_q + m_s), \tag{8}$$

where m_v, m_q, and m_s are the VWI quark masses. This was the form used to extrapolate for u/d and interpolate for s. The systematic error incorporates an estimate of sensitivity to nonlinear quark mass dependence made by adding a quadratic term as in Eq. (5). Also included in the systematic error are estimated uncertainties associated with radiative and discretization corrections to the NRQCD action.

The heavy-light meson results look quite reasonable although there is a systematic underestimate of the mass by about 25 MeV compared to experimental values. It is plausible that a common effect underlies this trend. At this stage, we do not know the effect of changing the lattice spacing so it is natural to suspect that the overall discrepancy in Table IV is due to a small uncorrected lattice spacing error. Assuming the lattice spacing error associated with the light quark action is $\mathcal{O}(a^2\Lambda_{\mathrm{QCD}}^2)$ one gets the estimate $a^2\Lambda_{\mathrm{QCD}}^2(\text{mass-}M_\Upsilon/2)$ $\sim$0.015 GeV which is roughly the size of the observed discrepancy. Note that for heavy-light mesons, where the wave functions are not so strongly affected by short distance interactions as in bottomonium, there is good agreement of the calculated spin splittings with experimental values.

B. Baryons

The calculation of baryon masses proceeds very much like that for heavy-light mesons. The simulation energies

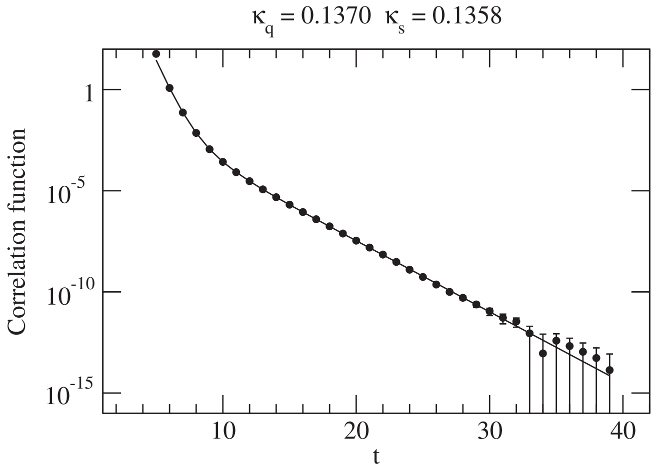

FIG. 1. A Σ_b correlator as a function of lattice time. The lattice boundaries are at t equals 1 and 40. The source is at t equals 5. The fit (solid line) is done including points t equals 6 to 32.

were determined by doing four-term exponential fits to the baryon correlation function. A typical example, showing the quality of the simulation data and of the fit, is given in Fig. 1. For single-b baryons, masses were calculated using the baryon analog of Eq. (7). The resulting masses were first interpolated in the b-quark mass to the physical point determined by M_Υ. Then the u/d and s-quark mass dependence was fit using Eq. (8). A linear quark mass dependence was consistent with all simulation data. A quadratic valence mass dependence was used to estimate a systematic uncertainty.

The results for single-b baryons are tabulated in Table V and plotted in Fig. 2 with statistical errors and in Fig. 3 with combined statistical and systematic errors. The Λ_b and Σ_b show significant sensitivity to the inclusion of a quadratic term in the mass fit; other masses are not changed very much by this term. The present results show a vast improvement in statistical precision compared to our previous study [1]. Multiexponential constrained fitting which uses time-correlation information over a large range, including times where the correlation function statistical errors are small, plays an important role in this improvement. Also shown in Table V is the quantity mass-$M_\Upsilon/2$. This is the actual quantity that the lattice simulation provides and, since most of the heavy hadron mass is due to the b-quark mass, it is a rough measure of the quark and gluon interaction energy. With the present analysis methods this quantity is determined to a few percent.

TABLE V. Lattice results for masses of single-b baryons (in GeV) compared to experimental values.

	mass-$M_\Upsilon/2$	mass	Experiment	Ref.
Λ_b	$0.911(21)(^{15}_{33})$	$5.641(21)(^{15}_{33})$	5.620(2)	[8]
Σ_b	$1.065(16)(^{17}_{26})$	$5.795(16)(^{17}_{26})$	5.8115(30)	[9]
Σ_b^*	$1.112(26)(^{20}_{18})$	$5.842(26)(^{20}_{18})$	5.8327(34)	[9]
Ω_b	$1.276(10)(^{20}_{19})$	$6.006(10)(^{20}_{19})$	6.165(16)	[10]
Ω_b^*	$1.314(18)(^{20}_{21})$	$6.044(18)(^{20}_{21})$		
Ξ_b	$1.051(17)(^{17}_{16})$	$5.781(17)(^{17}_{16})$	5.7929(30)	[11]
Ξ_b'	$1.173(12)(^{18}_{19})$	$5.903(12)(^{18}_{19})$		
Ξ_b^*	$1.220(21)(^{19}_{21})$	$5.950(21)(^{19}_{21})$		

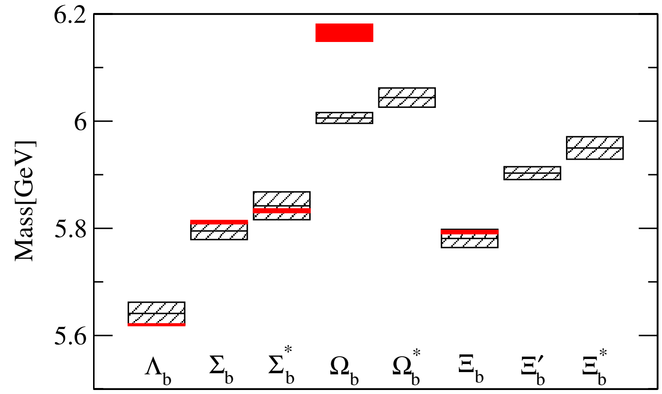

FIG. 2 (color online). Masses of single-b baryons. The diagonally-hatched boxes are lattice results with statistical errors only. Solid bars (red) are experimental values.

With the exception of Ω_b the results are in good agreement with the experimental values. However, one should not overinterpret this agreement since scaling (with lattice spacing) has not been checked and effects of using more realistic u/d quark masses still have to be considered.

The large discrepancy between our calculated Ω_b mass and the value reported in [10] is perplexing. To understand how puzzling it is, consider the basic physical idea behind heavy quark effective theory: a heavy quark acts essentially as a static color source and so mass differences between states with different light-quark configurations should be independent of heavy quark mass (up to corrections inversely proportional to the heavy mass). This suggests a direct data-to-data comparison of mass differences in single-charm and single-bottom baryons as shown in

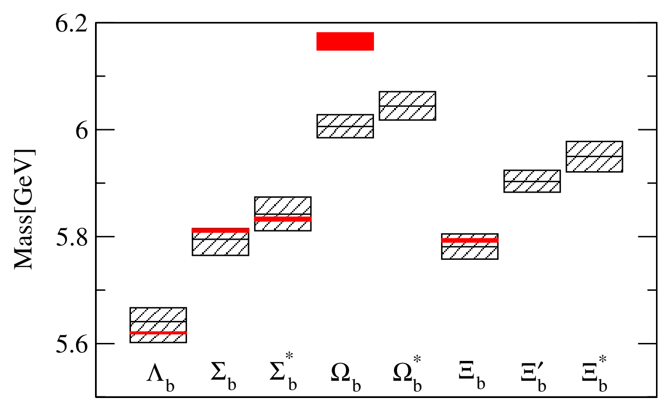

FIG. 3 (color online). Masses of single-b baryons. The diagonally-hatched boxes are lattice results with combined statistical and systematic errors. Solid bars (red) are experimental values.

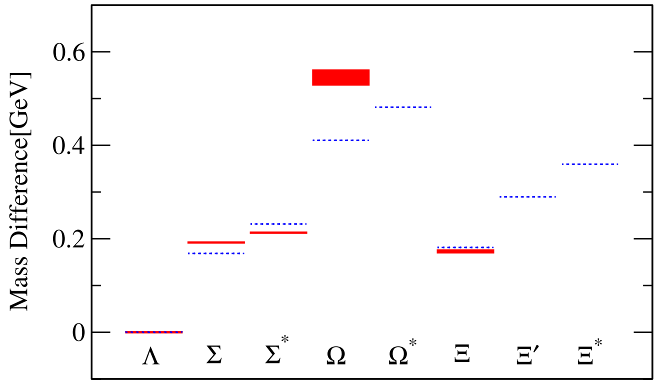

FIG. 4 (color online). Experimentally measured values of masses of single-charm (dashed, blue) and single-bottom baryons (solid, red) relative to the lowest lying state Λ.

Fig. 4. The measured masses of the singly-heavy Σ, Σ^* and Ξ baryons fit the expected pattern but Ω shows a large discrepancy, the same behavior as observed with our lattice simulation. The application of heavy quark effective theory to singly-heavy baryons was formalized by Jenkins [29]. In this work a combined expansion in the inverse of the heavy-quark mass, in $1/N_c$ and in SU(3) flavor symmetry breaking was carried out. Mass formulas were derived which then allow some masses to be predicted in terms of other experimentally measured masses. This is a more rigorous version of our data-to-data comparison. The updated predictions for single-b baryons from Jenkins [7] are shown in Fig. 5 along with our lattice results and the experimental values. There is consistency between our lattice results and the effective theory analysis of [7,29] across the whole spectrum which further accentuates the Ω_b puzzle.

The masses of double-b baryons are calculated using

$$M_{bb} = E_{\rm sim}^{(bb)} + M_\Upsilon - E_{\rm sim}^{(\Upsilon)}. \tag{9}$$

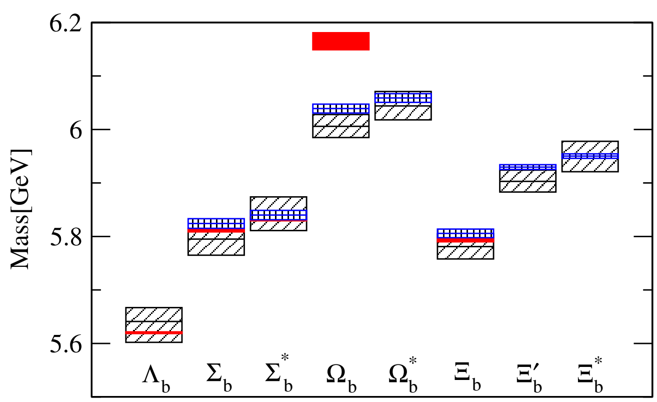

FIG. 5 (color online). Masses of single-b baryons from Jenkins [7] (vertically-hatched boxes, blue). The diagonally-hatched boxes are lattice results and solid bars (red) are experimental values.

TABLE VI. Lattice results for masses of double-b baryons (in GeV).

	mass-M_Υ	mass
Ξ_{bb}	$0.667(13)(^{12}_{26})$	$10.127(13)(^{12}_{26})$
Ξ^*_{bb}	$0.691(14)(^{16}_{25})$	$10.151(14)(^{16}_{25})$
Ω_{bb}	$0.762(9)(^{12}_{13})$	$10.225(9)(^{12}_{13})$
Ω^*_{bb}	$0.786(10)(^{18}_{12})$	$10.246(10)(^{18}_{12})$
$\Xi^*_{bb} - \Xi_{bb}$		$0.026(8)(^{11}_{10})$
$\Omega^*_{bb} - \Omega_{bb}$		$0.025(7)(^{11}_{6})$

The masses are interpolated and extrapolated as above. The final results are listed in Table VI and shown in Figs. 6 and 7 with statistical and combined errors, respectively. As yet there are no experimental values to compare with these calculations. The mass difference between spin 3/2 and spin 1/2 states in the doubly heavy sector is interesting because in the quark model and in heavy quark effective theory the baryon spin splitting can be related to the spin splitting for heavy-light mesons [30–33]. Simple arguments suggest that

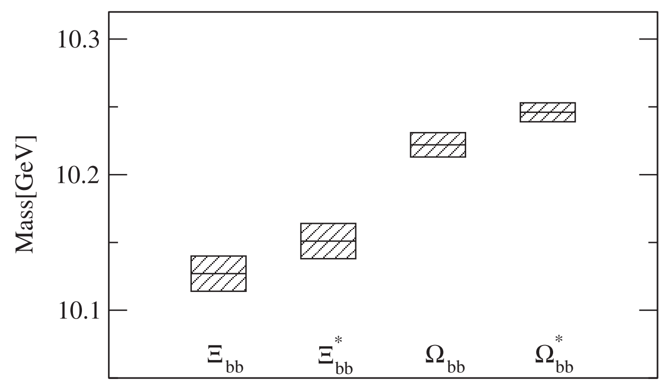

FIG. 6. Lattice results for masses of double-b baryons showing statistical errors only.

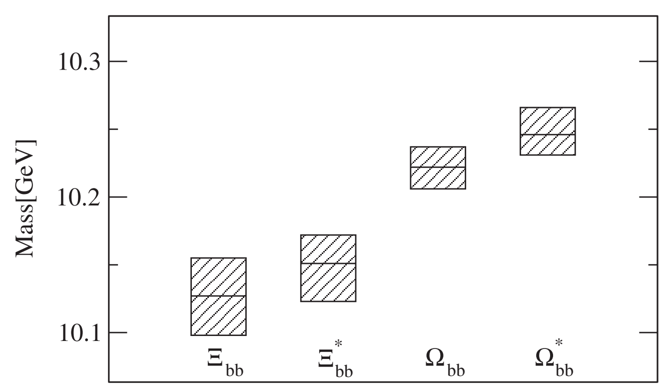

FIG. 7. Lattice results for masses of double-b baryons showing combined statistical and systematic errors.

$$\Delta M_{\text{baryon}} \approx \tfrac{3}{4}\Delta M_{\text{meson}}. \tag{10}$$

Within errors, our lattice spin splittings are consistent with this relation but are not precise enough to test it very stringently.

IV. SUMMARY AND DISCUSSION

In this paper the masses of bottom baryons were calculated in a 2 + 1 flavor dynamical lattice simulation. The clover action was used for light (u/d and s) quarks and the b quark was described by NRQCD. Using constrained multiexponential fitting for hadron correlators led to much more precise results than our previous studies. Single bottom baryons whose masses can be compared to experimental values show good agreement with the exception of the recently measured Ω_b.

The Ω_b is puzzling since our lattice result is consistent with ideas based on heavy quark effective theory which allow for a prediction of the Ω_b mass using only empirical input.

Predictions are made for the still unobserved single-b baryons and for the double-b baryons. Experimental observation of any of these states would be extremely interesting and might shed some light on the Ω_b puzzle.

This study should be considered as the first step in a program to do precision calculations in the heavy baryon sector. To go further, some systematic improvements have to be made. Radiative corrections to the NRQCD action are one of the major contributions to the systematic error and have to be dealt with. The light quark action is not corrected for lattice spacing errors to the same extent as the heavy quark action. Calculations are needed at more than one lattice spacing to enable a continuum extrapolation and to estimate reliably lattice spacing errors.

The present simulation is done in a region where the u/d quark masses are about 0.4 times the strange mass and some baryon masses exhibit a sensitivity to light quark mass extrapolation. Smaller values for the u/d mass would be highly desirable to insure that the simulation captures more accurately the dynamical sea-quark effects and that the extrapolation to the physical point can be put on a firm theoretical basis. Using an array of algorithmic improvements, the PACS-CS collaboration has produced configurations with the clover action pushing the light quark masses to near the physical region [34]. As of this writing, these configurations are not available for our use. Other fermion formulations could be considered, such as staggered fermions [35], domain-wall fermions [36], or twisted mass QCD [37] which presently operate at u/d to s-quark mass ratios as small as 0.1, 0.217, and 0.16, respectively. However, how to combine NRQCD with such approaches may require some attention. Also, the possibility of a hybrid calculation where sea and valence quarks are treated using different actions needs further consideration.

In our previous papers charmed baryons were also studied [1,32] and one would like to test one's capability of doing calculations in this sector. At the lattice spacing used here the charm quark is too light for NRQCD so the treatment of charmed baryons is left for future work.

ACKNOWLEDGMENTS

We thank the CP-PACS/JLQCD Collaborations for making their dynamical gauge field configurations available. Also, we thank Robert Petry for maintaining the VXRACK cluster at the University of Regina where our computations were done and Wendy Taylor for a discussion of the D0 Collaboration's Ω_b result. This work was supported in part by the Natural Sciences and Engineering Research Council of Canada.

APPENDIX

The heavy quark action is described using NRQCD [16]. The heavy quark propagator is given by

$$G_{\tau+1} = \left(1 - \frac{aH_B}{2}\right)\left(1 - \frac{aH_A}{2n}\right)^n \frac{U_4^\dagger}{U_0}\left(1 - \frac{aH_A}{2n}\right)^n \times \left(1 - \frac{aH_B}{2}\right)G_\tau, \tag{A1}$$

with $n = 5$ used in this work. The Hamiltonian is separated into two terms, $H = H_A + H_B$, with H_A containing the kinetic piece H_0 and the term proportional to c_{10} (defined below).

The Hamiltonian contains all terms up to $O(1/M_0^3)$ in the classical continuum limit:

$$H = H_0 + \delta H, \tag{A2}$$

$$H_0 = \frac{-\Delta^{(2)}}{2M_0}, \tag{A3}$$

$$\delta H = \delta H^{(1)} + \delta H^{(2)} + \delta H^{(3)} + O(1/M_0^4), \tag{A4}$$

$$\delta H^{(1)} = -\frac{c_4}{U_0^4}\frac{g}{2M}\boldsymbol{\sigma}\cdot\tilde{\mathbf{B}} + c_5\frac{a^2\Delta^{(4)}}{24M_0}, \tag{A5}$$

$$\delta H^{(2)} = \frac{c_2}{U_0^4}\frac{ig}{8M_0^2}(\tilde{\boldsymbol{\Delta}}\cdot\tilde{\mathbf{E}} - \tilde{\mathbf{E}}\cdot\tilde{\boldsymbol{\Delta}}) - \frac{c_3}{U_0^4}\frac{g}{8M_0^2}\boldsymbol{\sigma}\cdot(\tilde{\boldsymbol{\Delta}}\times\tilde{\mathbf{E}} - \tilde{\mathbf{E}}\times\tilde{\boldsymbol{\Delta}}) - c_6\frac{a(\Delta^{(2)})^2}{16nM_0^2}, \tag{A6}$$

$$\delta H^{(3)} = -c_1 \frac{(\Delta^{(2)})^2}{8M_0^3} - \frac{c_7}{U_0^4}\frac{g}{8M_0^3}\{\tilde{\Delta}^{(2)}, \boldsymbol{\sigma}\cdot\tilde{\mathbf{B}}\} - \frac{c_9 i g^2}{8M_0^3}\boldsymbol{\sigma}\cdot\left(\frac{\tilde{\mathbf{E}}\times\tilde{\mathbf{E}}}{U_0^8} + \frac{\tilde{\mathbf{B}}\times\tilde{\mathbf{B}}}{U_0^8}\right) - \frac{c_{10}g^2}{8M_0^3}\left(\frac{\tilde{\mathbf{E}}^2}{U_0^8} + \frac{\tilde{\mathbf{B}}^2}{U_0^8}\right) - c_{11}\frac{a^2(\Delta^{(2)})^3}{192n^2M_0^3}. \tag{A7}$$

The tildes indicate that the leading discretization errors have been removed. In particular,

$$\tilde{E}_i = \tilde{F}_{4i}, \tag{A8}$$

$$\tilde{B}_i = \tfrac{1}{2}\epsilon_{ijk}\tilde{F}_{jk}, \tag{A9}$$

where

$$\tilde{F}_{\mu\nu}(x) = \frac{5}{3}F_{\mu\nu}(x) - \frac{1}{6U_0^2}[U_\mu(x)F_{\mu\nu}(x+\hat{\mu})U_\mu^\dagger(x) + U_\mu^\dagger(x-\hat{\mu})F_{\mu\nu}(x-\hat{\mu})U_\mu(x-\hat{\mu}) - (\mu\leftrightarrow\nu)] + \frac{1}{3}\left(\frac{1}{U_0^2}-1\right)F_{\mu\nu}(x). \tag{A10}$$

The last term in $\tilde{F}_{\mu\nu}(x)$ corrects for the fact that the gauge field link multiplied by a tadpole factor is no longer unitary [38].

The spatial lattice derivatives are given by

$$a\Delta_i G(x) = \frac{1}{2U_0}[U_i(x)G(x+\hat{\imath}) - U_i^\dagger(x-\hat{\imath})G(x-\hat{\imath})], \tag{A11}$$

$$a\Delta_i^{(+)}G(x) = \frac{U_i(x)}{U_0}G(x+\hat{\imath}) - G(x), \tag{A12}$$

$$a\Delta_i^{(-)}G(x) = G(x) - \frac{U_i^\dagger(x-\hat{\imath})}{U_0}G(x-\hat{\imath}), \tag{A13}$$

$$a^2\Delta_i^{(2)}G(x) = \frac{U_i(x)}{U_0}G(x+\hat{\imath}) - 2G(x) + \frac{U_i^\dagger(x-\hat{\imath})}{U_0}G(x-\hat{\imath}), \tag{A14}$$

$$\tilde{\Delta}_i = \Delta_i - \frac{a^2}{6}\Delta_i^{(+)}\Delta_i\Delta_i^{(-)}, \tag{A15}$$

$$\Delta^{(2)} = \sum_i \Delta_i^{(2)}, \tag{A16}$$

$$\tilde{\Delta}^{(2)} = \Delta^{(2)} - \frac{a^2}{12}\Delta^{(4)}, \tag{A17}$$

$$\Delta^{(4)} = \sum_i (\Delta_i^{(2)})^2. \tag{A18}$$

[1] N. Mathur, R. Lewis, and R. M. Woloshyn, Phys. Rev. D **66**, 014502 (2002).
[2] H. Na and S. A. Gottlieb, Proc. Sci. LATTICE 2007 (2007) 124.
[3] T. Burch, C. Hagen, C. B. Lang, M. Limmer, and A. Schäfer, arXiv:0809.1103.
[4] X. Liu, H. X. Chen, Y. R. Liu, A. Hosaka, and S. L. Zhu, Phys. Rev. D **77**, 014031 (2008).
[5] M. Karliner and H. J. Lipkin, Phys. Lett. B **660**, 539 (2008).
[6] D. Ebert, R. N. Faustov, and V. O. Galkin, Phys. Lett. B **659**, 612 (2008).
[7] E. E. Jenkins, Phys. Rev. D **77**, 034012 (2008).
[8] W.-M. Yao *et al.*, J. Phys. G **33**, 1 (2006).
[9] T. Aaltonen *et al.* (CDF Collaboration), Phys. Rev. Lett. **99**, 202001 (2007).
[10] V. M. Abazov *et al.*, Phys. Rev. Lett. **101**, 232002 (2008).
[11] V. Abazov *et al.* (D0 Collaboration), Phys. Rev. Lett. **99**, 052001 (2007); T. Aaltonen *et al.* (CDF Collaboration), Phys. Rev. Lett. **99**, 052002 (2007).
[12] T. Ishikawa *et al.* (CP-PACS/JLQCD Collaborations), Proc. Sci. LAT2006 (2006) 181.
[13] T. Ishikawa *et al.* (CP-PACS/JLQCD Collaborations), Phys. Rev. D **78**, 011502 (2008).
[14] Y. Iwasaki, Nucl. Phys. **B258**, 141 (1985); Univ. of Tsukuba Report No. UTHEP-118, 1983.
[15] B. Sheikoleslami and R. Wohlert, Nucl. Phys. **B259**, 572 (1985).
[16] G. P. Lepage, L. Magnea, C. Nakhleh, U. Magnea, and K. Hornbostel, Phys. Rev. D **46**, 4052 (1992).
[17] http://www.jldg.org/index.html.
[18] S. Aoki *et al.*, Phys. Rev. D **73**, 034501 (2006).
[19] S. Aoki *et al.*, Phys. Rev. D **65**, 094507 (2002).
[20] R. Lewis and R. M. Woloshyn, Phys. Rev. D **58**, 074506 (1998).
[21] G. P. Lepage *et al.*, Nucl. Phys. B, Proc. Suppl. **106**, 12 (2002).
[22] A. Gray, I. Allison, C. T. H. Davies, E. Gulez, G. P. Lepage, J. Shigemitsu, and M. Wingate, Phys. Rev. D **72**, 094507 (2005).
[23] A. Manohar, Phys. Rev. D **56**, 230 (1997).

[24] B. Aubert *et al.* (*BABAR* Collaboration), Phys. Rev. Lett. **101**, 071801 (2008).
[25] H. D. Trottier, Phys. Rev. D **55**, 6844 (1997); N. H. Shakespeare and H. D. Trottier, Phys. Rev. D **58**, 034502 (1998).
[26] S. Collins *et al.*, Phys. Rev. D **60**, 074504 (1999).
[27] C. Stewart and R. Koniuk, Phys. Rev. D **63**, 054503 (2001).
[28] C. T. H. Davies and B. A. Thacker, Phys. Rev. D **45**, 915 (1992).
[29] E. E. Jenkins, Phys. Rev. D **54**, 4515 (1996).
[30] H. J. Lipkin, Phys. Lett. B **171**, 293 (1986).
[31] M. J. Savage and M. B. Wise, Phys. Lett. B **248**, 177 (1990).
[32] R. Lewis, N. Mathur, and R. M. Woloshyn, Phys. Rev. D **64**, 094509 (2001).
[33] D. Ebert, R. N. Faustov, V. O. Galkin, and A. P. Martynenko, Phys. Rev. D **66**, 014008 (2002); N. Brambilla, A. Vairo, and T. Rösch, Phys. Rev. D **72**, 034021 (2005); S. Fleming and T. Mehen, Phys. Rev. D **73**, 034502 (2006).
[34] S. Aoki *et al.*, arXiv:0807.1661.
[35] C. Bernard *et al.*, Proc. Sci. Lattice 2007 (2007) 090.
[36] C. Allton *et al.*, Phys. Rev. D **76**, 014504 (2007).
[37] B. Blossier *et al.*, J. High Energy Phys. 04 (2008) 020.
[38] S. Groote and J. Shigemitsu, Phys. Rev. D **62**, 014508 (2000).